

Origin of M2 M ϕ and its macrophage polarization by TGF- β in a mice intervertebral injury model

International Journal of
Immunopathology and Pharmacology
Volume 36: 1–11
© The Author(s) 2022
Article reuse guidelines:
sagepub.com/journals-permissions
DOI: 10.1177/03946320221103792
journals.sagepub.com/home/iji


Ayumu Kawakubo¹, Masayuki Miyagi¹, Yuji Yokozeki¹, Mitsufumi Nakawaki¹, Shotaro Takano¹, Masashi Satoh², Makoto Itakura³, Gen Inoue¹, Masashi Takaso¹ and Kentaro Uchida¹ 

Abstract

Introduction: Studies have identified the presence of M1 and M2 macrophages (M ϕ) in injured intervertebral discs (IVDs). However, the origin and polarization-regulatory factor of M2 M ϕ are not fully understood. TGF- β is a regulatory factor for M2 polarization in several tissues. Here, we investigated the source of M2 M ϕ and the role of TGF- β on M2 polarization using a mice disc-puncture injury model.

Methods: To investigate the origin of M2 macrophages, 30 GFP chimeric mice were created by bone marrow transplantation. IVDs were obtained from both groups on pre-puncture (control) and post-puncture days 1, 3, 7, and 14 and CD86 (M1 marker)- and CD206 (M2 marker)-positive cells evaluated by flow cytometry ($n = 5$ at each time point). To investigate the role of TGF- β on M2 polarization, TGF- β inhibitor (SB431542) was also injected on post-puncture days (PPD) 5 and 6 and CD206 expression was evaluated on day 7 by flow cytometry ($n = 5$) and real time PCR ($n = 10$).

Results: The proportion of CD86⁺ M ϕ within the GFP⁺ population was significantly increased at PPD 1, 3, 7, and 14 compared to control. CD206-positive cells in GFP-populations were significantly increased on PPD 7 and 14. In addition, the percentage of CD206-positive cells was significantly higher in GFP-populations than in GFP⁺ populations. TGF- β inhibitor reduced CD206-positive cells and *Cd206* expression at 7 days after puncture.

Conclusion: Our findings suggest that M2 M ϕ following IVD injury may originate from resident M ϕ . TGF- β is a key factor for M2 polarization of macrophages following IVD injury.

Keywords

Macrophages, resident, TGF- β

Date received: 16 April 2021; accepted: 11 May 2022

¹Department of Orthopedic Surgery, Kitasato University School of Medicine, Sagamihara, Japan

²Department of Immunology, Kitasato University School of Medicine, Sagamihara, Japan

³Department of Biochemistry, Kitasato University School of Medicine, Sagamihara, Japan

Corresponding author:

Kentaro Uchida, Department of Orthopedic Surgery, Kitasato University School of Medicine, 1-15-1 Minami-ku, Kitasato, Sagamihara 252-0374, Japan.

Email: kuchida@med.kitasato-u.ac.jp



Creative Commons Non Commercial CC BY-NC: This article is distributed under the terms of the Creative Commons Attribution-NonCommercial 4.0 License (<https://creativecommons.org/licenses/by-nc/4.0/>) which permits non-commercial use, reproduction and distribution of the work without further permission provided the original work is attributed as specified on the SAGE and Open Access pages (<https://us.sagepub.com/en-us/nam/open-access-at-sage>).

Introduction

Pathology of intervertebral discs (IVDs) is a major factor in chronic low back pain (LBP). A number of studies have reported finding macrophages (M ϕ) within IVDs with degeneration, indicating that M ϕ play a pivotal role in the pathology of IVD.^{1–3} Therefore, a better understanding of macrophage-mediated IVD pathology will aid the development of therapeutic strategies.

M ϕ have been functionally divided into two polarizing phenotypes, inflammatory M1 and anti-inflammatory M2. We previously reported that M1 M ϕ increased following IVD injury and made a contribution to inflammatory cytokine production and pain-associated molecules.^{4–6} Using green fluorescence protein (GFP)-bone marrow (BM) chimeric mice, we previously reported that BM-derived monocytes recruited to injured disc were the polarized M1 phenotype.⁷ In contrast, M2 M ϕ phenotypes have also been found in murine and human IVDs.^{1,6,8} However, the origin of M2 M ϕ and the mechanism of M2 polarization have not been determined.

Previous studies focused on the recruitment of M ϕ from BM following tissue injury because these cells often occur in greater numbers than resident M ϕ and exhibit inflammatory phenotypes during inflammation.^{7,9,10} However, several studies have identified the presence of resident M ϕ in several tissues, including adipose tissue and skeletal muscle,^{11,12} some of which exhibit an M2-like phenotype.^{13,14} We previously reported that F4/80+CD11b+ cells exist in intact IVDs containing nucleus pulposus (NP) and at annulus fibrosis (AF) using flow cytometric analysis.⁶ When intact IVD-derived CD11b+ cells were stimulated with IL-4 and IL-10 in vitro, expression of the M2 macrophage markers CD206 and Fizz1 was elevated.⁷ A more recent study showed that F4/80+ cells were localized at annulus fibrosis (AF) of mice intact IVD.¹⁵ We therefore hypothesized that M2 M ϕ originate from resident M ϕ .

Transforming growth factor-beta (TGF- β) signaling plays an essential role in the development and tissue homeostasis of the IVD.¹⁶ Previous studies reported that TGF- β expression was increased in mice and human degenerative IVD^{17–20} and that exogenous TGF- β treatment suppressed IVD inflammation in vitro and in vivo.^{21–23} In contrast, other studies indicated that TGF- β plays a key role in M2 polarization of macrophages within the tumor environment.^{24,25} However, the role of TGF- β in M2 polarization in IVD remains unclear.

Here, we investigated the origin of M2 M ϕ polarization following IVD injury and role of TGF- β on M2 polarization following IVD injury in mice.

Methods

Animals

The protocol was approved by Kitasato Institutional Animal Care Committee (reference number: 2020-089). The

study was performed in compliance with the ARRIVE guidelines for reporting of animal experiments. All methods were performed in accordance with guidelines for the conduct of animal experimentation from the Science Council of Japan. Male C57BL/6J (B6) mice and GFP-transgenic (GFP-tg) mice were used at age 10 weeks. The mice were maintained in a housing system kept at $25 \pm 1^\circ\text{C}$ with $60 \pm 5\%$ humidity and a 12:12 hour light–dark cycle. The study protocol was approved by our institution's Animal Care Committee (reference no.: 2020-089). Sample size for PCR analysis was determined based on our previous studies.^{6,26} Power analysis with an alpha of 0.05 and power of 0.80 was conducted using G*POWER3 to determine a sufficient sample size for each analysis, except PCR analysis. IVDs were resected without separating the NP and AF, and pooled for each experiment.

Generation of GFP BM chimeric mice

To distinguish bone marrow-derived macrophages and resident macrophages, GFP BM chimeric mice were generated. Following induction of anesthesia using isoflurane, an anesthesia cocktail containing butorphanol tartrate, medetomidine hydrochloride, and midazolam was injected via intramuscular injection in an upper limb of mice. BM cells from 15 male GFP-tg mice were injected into the tibia of 30 recipient B6 mice which had received 10.5 Gy irradiation from a cesium source.⁷ We previously reported that BM transplantation following 10.5 Gy irradiation was able to replace almost all peripheral blood cells (approximately 97%) for 4 weeks after transplantation.⁷ Therefore, 4 weeks after BM transplantation, five of the 30 mice were randomly grouped as the control group, in which IVDs were not disturbed, and the remaining 25 mice were used as the IVD injury group, in which a 27-gauge needle was employed for puncture of IVDs (coccygeal discs 5–6 and 6–7) a total of 10 times. On pre-puncture (control) and post-puncture days 1 (PPD 1), 3 (PPD 3), 7 (PPD 7), and 14 (PPD 14), IVDs were obtained from the two groups for evaluation with flow cytometry ($n = 5$ per time point).

Flow cytometric analysis

To clarify the difference in the ratio of CD206-positive cells (%) between GFP+ and GFP– cells at PPD 7 and PPD 14, preliminary data ($n = 3$), including mean (PPD 7, GFP–, 0.300, GFP+, 0.070; PPD 14, GFP–, 0.214, GFP+, 0.034) and standard deviation (PPD 7, GFP–, 0.095, GFP+, 0.054; PPD 14, GFP–, 0.100%, GFP+, 0.036), were entered into G*POWER3. Power analysis revealed that 4 samples for PPD 7 and 5 samples for PPD 14 were needed to detect a difference between GFP– and GFP+ cells. Accordingly, IVDs were obtained from 30 mice ($n = 5$ at each time point). IVDs were digested with 2 mg/mL collagenase type I

Table 1. Primer Sequences.

Primer	Sequence (5'–3')	Product size (bp)
<i>Cd206-F</i>	TGGCAATTCAGGAGAGGCAG	109
<i>Cd206-R</i>	AGTGGTTGGAGAAACAGGCA	
<i>Tgfb-F</i>	CTCCCGTGGCTTCTAGTGC	133
<i>Tgfb-R</i>	GCCTTAGTTTGGACAGGATCTG	
<i>Fizz1-F</i>	ACTGCTACTGGGTGTGCTTG	101
<i>Fizz1-R</i>	GCAGTGGTCCAGTCAACGA	
<i>Gapdh-F</i>	AACTTTGGCATTGTGGAAGG	223
<i>Gapdh-R</i>	ACACATTGGGGGTAGGAACA	

solution overnight at 37°C, and filtered through a nylon mesh filter with a pore size of 100 µm to obtain single-cell suspensions. IVD-derived cells were incubated with anti-CD45 (conjugated with PE/Cy7, Clone: 30-F11), anti-F4/80 (conjugated with BV421TM, Clone: RM8), anti-CD11b (conjugated with APC-Cy7, Clone: M1/70) antibodies for 50 min at 4°C then treated with a fixation/permeabilization solution (BioLegend). Then, the cells were reacted with CD86 (conjugated APC antibody, Clone: GL-1) or CD206 (conjugated APC antibody, Clone: C068C2) at 4°C for 30 min. After two washings in washing buffer, a total of 30,000 events were provided via the BD FACSVerse system (BD Biosciences, San Jose CA, USA) and the findings were evaluated with FlowJo v10.7TM (Tree Star, Ashland OR, USA). Negative gates were obtained using the isotype control.

TGF-β expression and localization in the IVD injury model

Sample size ($n = 10$) for PCR analysis of TGF-β was determined based on our previous study.⁶ To clarify the difference in TGF-β protein concentration (µg/mg total protein) between control and PPD 7, preliminary data ($n = 5$) including mean (control, 1.48; PPD 7, 1.75) and standard deviation (control, 0.21; PPD 7, 0.18) were entered into G*POWER3. Power analysis revealed that 10 samples were needed to detect a difference between control and PPD 7 for ELISA. Fifty male B6 mice were used to create a puncture model, as described above. IVDs were obtained at control ($n = 25$), PPD 1 ($n = 20$), PPD 3 ($n = 20$), PPD 7 ($n = 25$), and PPD 14 ($n = 20$). *Tgfb* mRNA and TGF-β protein expression was analyzed by real time PCR and ELISA, respectively ($n = 10$ at each time point). TGF-β localization at control and PPD 7 was evaluated by immunohistochemistry ($n = 5$).

Real time PCR analysis

Following treatment, total RNA was obtained from cells with the standard Trizol/chloroform method. First-strand

cDNA was synthesized with superscript III RTTM (Invitrogen, Carlsbad CA, USA) and analyzed by real time PCR with the SYBRTM green method (Qiagen, Valencia CA, USA). Mouse M2 markers *Cd206* and *Fizz1* were examined with reference to previous reports. Primers were all synthesized with reference to our previous reports^{6,8} (Table 1). The delta–delta Ct method was utilized with the housekeeping gene *Gapdh* to evaluate relative mRNA levels in comparison with vehicle.

Immunohistochemistry

To determine TGF-β localization, IVD samples from control and PPD 7 were paraffin-embedded and sliced into 4 µm sections. The sections were deparaffinized for 1 h with xylene, then hydrated in a serial dilution of ethanol (100%, 95%, and 70%) and rinsed in distilled water. Exogenous peroxidase was blocked by incubating the sections with 3% hydrogen peroxide for 15 min in methanol. The slides were then washed with phosphate-buffered saline (PBS) and incubated with 10% goat serum (Nichirei, Tokyo, Japan) at room temperature. Subsequently, they were incubated with anti-TGF-β monoclonal rabbit IgG (category number: ab215715, Abcam, Cambridge, MA) for 2 h at room temperature. Location of the primary antibodies was determined using the streptavidin-biotin-peroxidase method (Histofine SAB-PO Kit; Nichirei, Tokyo, Japan). All sections were counterstained using Meyer's hematoxylin. Sections without incubation with primary antibody were used as control.

ELISA

IVD samples obtained from control, PID1, PID3, PID 7, and PPD 14 were subject to homogenization in RIPA buffer which contained protease inhibitor cocktails with a Polytron homogenizer. The homogenates were subject to centrifugation at 15,000 r/min for 5 min at 4°C. Protein concentration was analyzed by BCA assay and prepared at the concentration of 250 µg/ml. TGF-β concentration was estimated using a commercial mouse TGF-β ELISA kit (R&D Systems, Minneapolis, MN, USA).

Effect of TGF- β on disc macrophage in vitro

IVDs were obtained from five mice and digested with 2 mg/mL type I collagenase at 37°C for 18 h, then strained through a 100 μ m filter ($n = 5$). Obtained cells incubated in biotinylated anti-CD11b antibody at 4°C for 30 min. The cells were first washed with PBS and mixed with streptavidin-labeled magnetic particles, then subject to incubation on ice for 30 min using an IMag separation system (BD Biosciences). Following removal of unbound (CD11b-negative) cells, the tub was detached from the magnetized support and a further 2 mL α -MEM which contained 10% fetal bovine serum was added to obtain CD11b-positive cells. The CD11b-positive disc-derived macrophages were cultured with α -MEM supplemented with 100 ng/mL mouse recombinant macrophage colony stimulating factor (mrM-CSF). Previous studies used TGF- β stimulation of M2 polarization when macrophages were incubated with IL-10 in vitro.^{26,27} In addition, TGF- β stimulation in the absence of IL-10 failed to induce CD206 in disc macrophages (Supplemental Figure 1). Therefore, disc macrophages were stimulated in culture medium (vehicle), 10 ng/mL mouse recombinant TGF- β (mrTGF- β , R&D System) and 10 ng/mL IL-10, mrTGF- β + IL-10 + 1 μ M SB431542 (TGF- β inhibitor) for 30 min, at which time phosphorylation of SMAD2 and SMAD3 was evaluated by western blotting. After stimulation for 24 h, M2 marker (*Cd206*, *Fizz1*) was evaluated by real time PCR analysis

Western blotting

Disc-derived macrophages were stimulated using culture medium (vehicle), mrTGF β , mrTGF β + SB431542 for 30 min. The cells were subsequently lysed with sodium dodecyl sulfate (SDS) sample buffer, and proteins contained in the lysates (5 μ g) were separated by SDS polyacrylamide gel electrophoresis, followed by electrophoretic transfer to a polyvinylidene difluoride membrane in a blotting buffer. The membrane was then subject to blocking using 10% nonfat milk added to Tris-buffered saline which contained 0.05% Tween 20 (TBS-T) at RT for 1 h. Following blocking, the membrane was then reacted with anti-SMAD2 rabbit monoclonal antibody (1: 1000; Cell Signaling Technology, Inc., Danvers, MA, USA), anti-phosphor-SMAD2 (Ser465/467) rabbit monoclonal antibody (1: 10,000 Cell Signaling Technology), anti-SMAD3 rabbit monoclonal antibody (1: 1000; Cell Signaling Technology, Inc.), anti-phosphor-SMAD3 (Ser423/425) rabbit monoclonal antibody (1:1000; Cell Signaling Technology, Inc.), anti-SMAD4 (1:1000; Cell Signaling Technology, Inc.), and GAPDH (1:5000; Cell Signaling Technology, Inc) for 1 h at RT. It was then reacted with HRP-conjugated goat anti-rabbit IgG antibody for a further hour. After three rinses

using TBS-T, proteins on the membrane were detected by enhanced chemiluminescent detection with an ImageQuant LAS-4000mini (Fuji Photo Film Co). Densitometry of the western blot protein bands was analyzed using ImageJ and findings were normalized to those of GAPDH.

Effect of TGF- β inhibitor on M2 macrophage marker expression in IVD injury models

In the puncture model, elevated gene and protein expression of TGF- β - and CD206-positive cells was observed at PPD 7. Therefore, we evaluated the effect of TGF- β inhibition at PPD 7. Power analysis based on preliminary data ($n = 3$) revealed that 5 samples were needed to detect a difference of CD206-positive cells between the vehicle (mean, 0.24; SD, 0.075) and SB431542 groups (mean, 0.12; SD, 0.01). Accordingly, five mice in each group were used for flow cytometric analysis. Sample size ($n = 10$) for PCR analysis of *Cd206* was determined based on our previous study.²⁶ The puncture model was created in 30 C57BL/6J mice, with random and equal assignment to the vehicle or treatment groups. One group received intraperitoneal (IP) injection with 10 mg/kg SB431542 in a 5% DMSO solution while the second received IP injection with 5% DMSO solution (vehicle) at PPD 5 and PPD 6. Dose was determined using the optimal inhibitory effect of 10 mg/kg on intraperitoneal administration, as reported previously.^{28,29} Five of the 10 mice in each group were used to analyze CD206+ M ϕ for flow cytometric analysis. The remaining mice were used to evaluate *Cd206* and *Fizz1* for qPCR analysis.

Statistical analysis

Tukey multiple comparison test was employed to identify day(s) showing differences in expression in the groups. Further, the t test was used to identify per-day differences between the groups.

Results

Proportion of CD86+ and CD206+ macrophages in GFP- and GFP+ cells after IVD injury

CD11b+F4/80+ (M ϕ) cells within IVD were increased at PPD 3, 7, and 14 compared to control (Figure 1, PPD 3, $p < .001$; PPD 7, $p = .010$; PPD 14, $p < .001$). CD86+ cells within IVD were increased at PPD 3 compared to control (Figure 1, PPD3, $p = .006$). CD206+ cells within IVD were increased at PPD 7 and PPD 14 compared to control (Figure 1, PPD 7, $p < .001$; PPD 14, $p = .008$). CD206/CD86 ratio was significantly reduced at PPD 3 ($p = .018$), but returned to baseline at PPD 7 and PPD 14.

The proportion of CD86+ M ϕ within the GFP+ population was significantly increased at PPD 1, 3, 7, and 14 compared to control (Figure 2a-f, PPD1, $p = .032$; PPD3, p

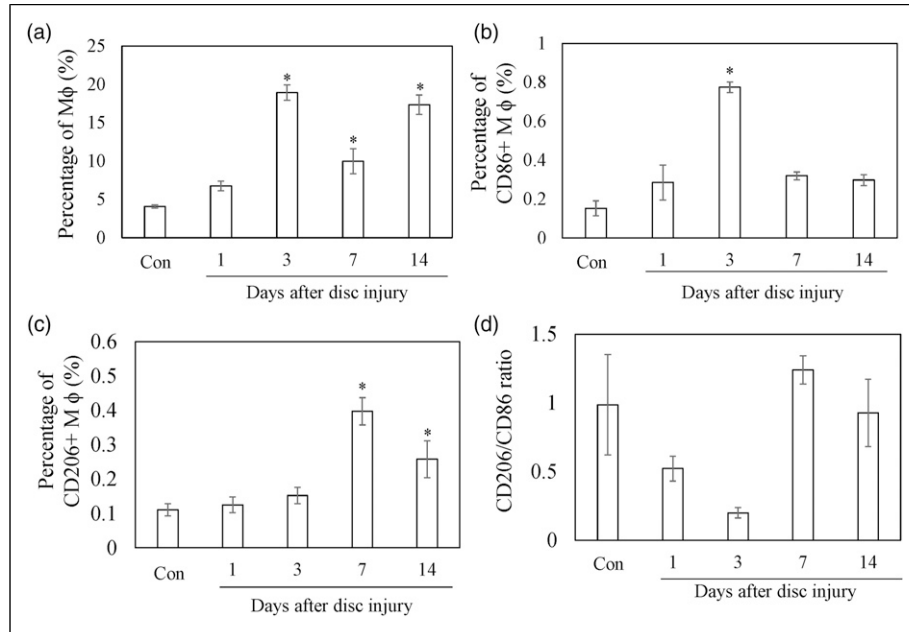


Figure 1. Flow cytometry analysis of the M1 and M2 macrophage population after intervertebral injury. Percentage of Mφ (CD11b+F4/80+) (a), CD86+Mφ (b), and CD206+Mφ (c) in IVDs. Ratio of CD206+/CD86+ (d). All data show the mean \pm standard error ($n = 5$). *, $p < .05$ in comparison with control (Con).

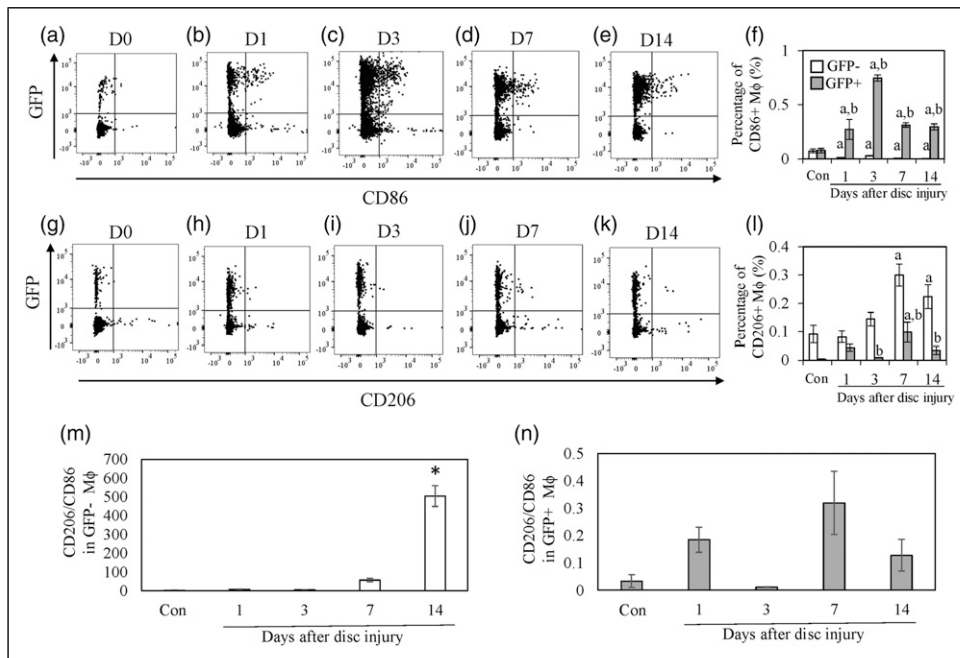


Figure 2. Ratio of M1 and M2 macrophages in GFP- and GFP+ cells. A–E. Dot plots of GFP+ and GFP- CD86+ cells in the intervertebral discs (IVDs). The X-axis indicates CD11b and the y-axis indicates green fluorescence protein (GFP). F. Percentage of CD86+ GFP- negative (white) and -positive (gray) cells in IVDs. G–K. Dot plots of GFP+ and GFP- CD206+ cells in IVDs. L. Percentage of CD206+ GFP- negative (white) and -positive (gray) cells in IVDs. All data represent mean \pm standard error ($n = 5$). A, $p < .05$ compared with control (Con); b, $p < .05$ compared with the time-matched GFP- population.

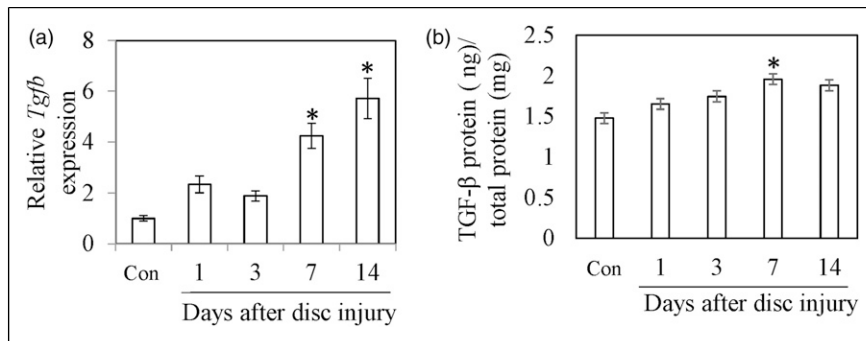


Figure 3. Expression of TGF- β after IVD injury. *Tgfβ* expression in IVDs (a). TGF- β protein concentration in IVDs (b). All data represent mean \pm standard error ($n = 10$).

*, $p < .05$ compared with control (Con).

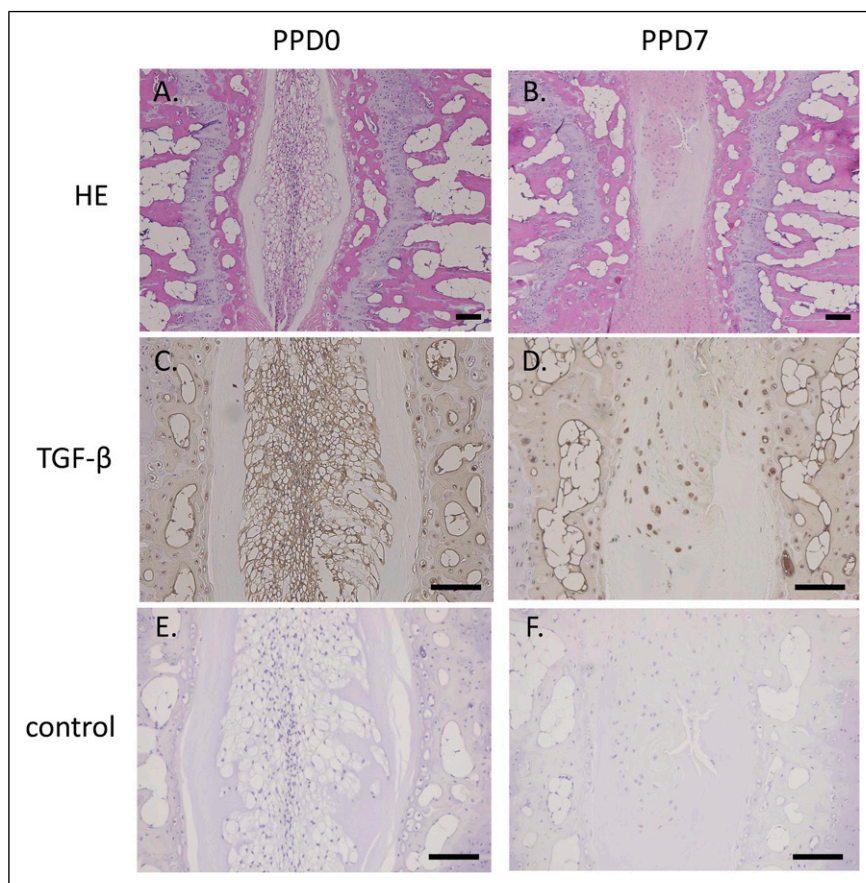


Figure 4. Localization of TGF- β following IVD injury. Hematoxylin and eosin-stained tissue sections of IVDs in the control (a) and injury groups (b) at post injury day 7. Immunostaining for *TGFβ* in the control (c) and injury groups (d) at post injury day 7. Negative control section without primary antibody in the control (e) and injury groups (f). Scale bar = 100 μ m.

$< .001$, PPD 7, $p = .009$; PPD 14, $p = .015$). In contrast, CD86⁺ M ϕ in the GFP⁻ population was significantly decreased at PPD 1, 3, 7, and 14 compared to control (Figure 2a–f, PPD 1, $p < .001$; PPD 3, $p = .006$; PPD 7, $p < .001$; PPD 14, $p < .001$). The proportion of CD86⁺CD11b+F4/80⁺ cells within the GFP⁺ population

was significantly greater than that in the GFP⁻ population at PPD 3, 7, and 14 (Figure 2a–f, PPD 3, $p < .001$; PPD 7, $p = .001$; PPD 14, $p = .002$) The percentage of CD206⁺ M ϕ was significantly increased within the GFP⁻ population at PPD 7 and 14 compared to control (Figure 2g–i, PPD 7, $p = .001$; PPD 3, $p < .001$; PPD 14, $p = .038$). The

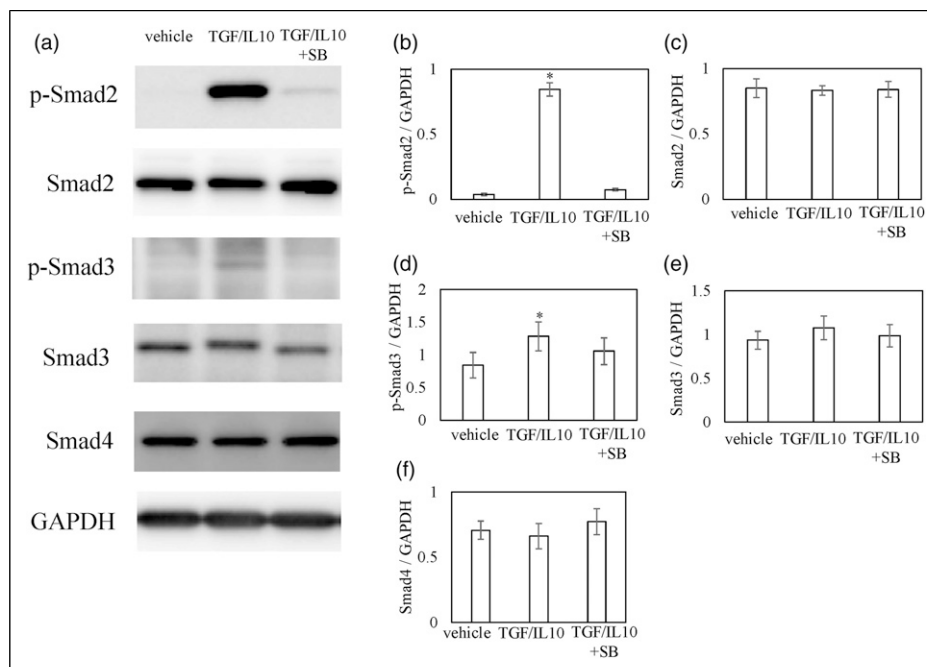


Figure 5. Effect of TGF- β on Smad pathway in vitro. Effects of TGF- β and TGF- β inhibitor on phosphorylation of smad2, smad3, smad4, and M2 maker (*Fizz1* and *Cd206*) mRNA expression. Disc macrophages (DMs) were exposed to α -MEM (control), 10 ng/mL mouse recombinant (mh) TGF- β + 10 ng/mL IL-10 (TGF/IL-10), or 10 ng/mL rhTGF- β + 10 ng/mL IL-10 + 10 μ M SB431542 (TGF/IL-10/SB) for 30 min before protein extraction and western blot. Grouping of gels/blots cropped from different parts of the same gel or obtained from different gels. Western blotting for phosphorylated smad2 (p-smad2), smad2, p-smad3, smad3, smad4, and GAPDH (a). Densitometry of western blot protein bands for p-smad2 (b), smad2 (c), p-smad3 (d), smad3 (e), and smad4 (f) were normalized to the expression of GAPDH. Data indicate mean \pm SE ($n = 5$).

* $p < .05$ in comparison with control.

percentage of CD206+ M ϕ cells was also significantly greater in the GFP+ population at PPD 7 ($p = .007$). However, the percentage of CD206+ M ϕ cells within the GFP- population was significantly increased compared to the percentage in the GFP+ population at PPD 3, 7, and 14 (Figure 2g-1, PPD 3, $p = .011$; PPD 7, $p = .011$; PPD 14, $p = .010$). CD206/CD86 ratio was significantly increased compared to the control at PPD 14 in the GFP- population (Figure 2m, $p < .011$). There was no difference in CD206/86 ratio in the GFP+ population among the groups (Figure 2n)

Expression and distribution of TGF- β following IVD injury

Tgfb mRNA expression was significantly increased at PPD 7 ($p < .001$) and PPD 14 (Figure 3a, $p < .001$). TGF- β protein concentration was also significantly increased at PPD 7 (Figure 3b, $P = .011$). There was no significant difference between control and PPD 1 ($p = 1.000$), PPD 3 ($p = .573$), or PPD14 ($p = .051$). The nucleus pulposus region in control was replaced by chondrocytic cells at PPD

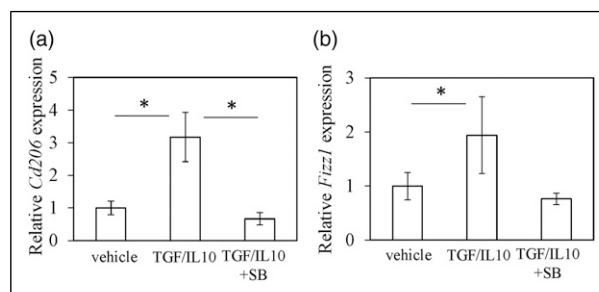


Figure 6. Effect of TGF- β on M2 maker expression in vitro. RT-PCR for *Cd206* (A) and *Fizz1* (B). DMs were exposed to the α -MEM control, TGF/IL-10, or TGF/IL-10/SB for 24 h. Relative expression was evaluated with regard to expression in the control samples. The data show mean \pm SE ($n = 5$).

* $p < .05$ in comparison with control.

7 (Figure 4a and b). TGF- β immunoreactivity was observed at both control and PPD 7. However, chondrocytic cells at PPD 7 were more heavily stained for TGF- β than intact IVD (Figure 4c and d). No TGF- β -positive cells were observed in control sections.

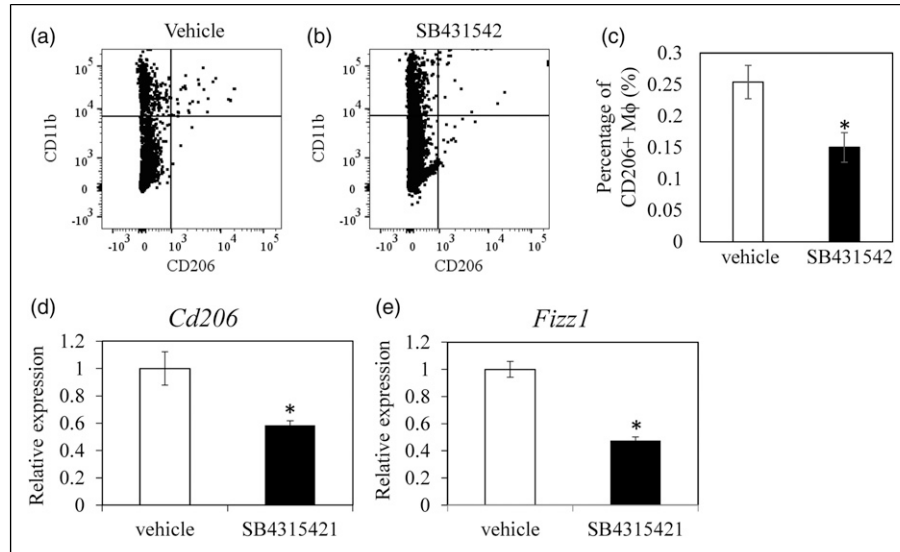


Figure 7. Effect of TGF- β inhibitor on M2 marker expression in vivo. Dot plots of CD11b+CD206+ cells in vehicle (DMSO)- and TGF- β inhibitor (SB435124)-treated groups (a). Ratio of CD11b+CD206+ cells in vehicle (DMSO)- and TGF- β inhibitor (SB435124)-treated groups ($n = 5$ for each group) (b). Expression of *Cd206* (c) and *Fizz1* (d) expression in vehicle (DMSO)- and TGF- β inhibitor (SB435124)-treated groups ($n = 10$ for each group). The data show mean \pm standard error. * $p < .05$ in comparison with vehicle.

Effect of TGF- β inhibition on M2 polarization in vitro

TGF- β /IL-10 induced the phosphorylation of Smad2 and Smad3 (Figure 5a–e), which was suppressed in the presence of SB431542 (Figure 5a–e). There were no changes in Smad4 expression in the presence of TGF- β /IL-10. Expression of M2 macrophage marker *Cd206* was significantly increased after TGF- β /IL-10 stimulation in DM (Figure 6a, *Cd206*, $p = .020$), while exposure to SB431542 significantly decreased this increase (Figure 6a, *Cd206*, $p = .015$). Although *Fizz1* increased after TGF- β /IL-10, no significant difference was seen among the groups (Figure 6b).

Effect of TGF- β inhibition on M2 polarization in vivo

Flow cytometric analysis showed that CD206+ macrophage was significantly reduced following SB431542 treatment (Figure 7a–c, *Cd206*, $p = .019$). *Cd206* and *Fizz1* expression at PPD 7 were significantly reduced following SB431542 treatment (Figure 7d and e, *Cd206*, $p = .009$; *Fizz1*, $p < .001$).

Discussion

M2-like M ϕ are related to the role of M ϕ in resolving inflammation, as well as in the induction and maintenance of homeostasis.^{9,14} Recent studies also suggest that recruited and tissue-resident M ϕ are independently regulated during inflammation.^{9,13} Tissue-resident M ϕ in peritoneum, lung, and brain are maintained by a self-renewing

and proliferative capacity even after exposure to an inflammatory environment. Tissue-resident M ϕ repopulate inflamed tissues in response to M-CSF and are not replenished by recruited monocytes.⁹ Our previous study indicated that CD86⁺ M1 macrophages increased in the acute phase of tissue inflammation, and mainly consisted of recruited (GFP+) macrophages.⁷ In our present study, resident macrophages polarized to M2 phenotype, CD206+ M ϕ . GFP+CD206+ macrophages were also increased at 7 days after injury, albeit in a significantly lower percentage than that of GFP-CD206-macrophages. Our results suggest that M2 M ϕ may predominantly originate from resident macrophages in disc.

Previous studies reported the macrophage subsets contribute to inflammation (M1), anti-inflammation (M2a), and tissue remodeling phenotype (M2c).^{30–33} Our previous study showed that stimulation of M1 polarization by IFN- γ and LPS increased CD86 expression in mouse bone marrow- and disc-derived CD11b-positive cells in vitro.⁷ In contrast, stimulation of M2a polarization by IL-4 promoted *Fizz1* and CD206 and M2c polarization by increased CD206 expression in disc-derived CD11b cells.⁷ Therefore, CD86 was used as marker for the inflammatory subset, M1 macrophage. *Fizz1* and CD206 were used as M2a and M2a+M2c markers, respectively. However, the specific function of CD86⁺ and CD206+ macrophages in IVDs remains unclear. In addition, a previous study reported that NP cells in human IVD express a macrophage/phagocytic cell marker, CD68.³⁴ In our study, we could not exclude the possibility that GFP-F4/80+CD11b+ were NP cells expressing macrophage markers.

Further functional and histological analysis of CD86 and CD206+ cells in IVD is needed.

A previous study reported that TGF- β increased the degree of degeneration in IVDs.³⁵ Similarly, increased TGF- β was observed in injured IVDs. In contrast, previous studies showed that TGF- β regulates the proliferation and polarization of resident macrophages.^{11,36} Additionally, the number of Langerhans cells (LC), resident macrophages in skin, decreases when TGF- β is absent.³⁶ Alveolar macrophages are significantly reduced in mice with conditional knockout of TGF receptors.¹¹ In our present study, TGF- β increased *Cd206* expression in mice disc macrophages in vitro. In addition, TGF- β inhibitor reduced CD206+ cells and suppressed the expression of *Cd206* in mice IVD puncture models. A previous study reported that TGF- β -polarized M2 macrophages exhibit an anti-inflammatory phenotype.²⁷ TGF- β may play a role in M2 polarization in the switch from an inflammatory process toward resolution during IVD injury.

Studies have reported that the relationship between TGF- β from different sources modulates M2 macrophages. Tumor cell-secreted TGF- β induces M2-type polarization of macrophages.³⁷ M2 macrophages secrete TGF- β in fibrotic disorders. We previously reported that TGF- β is dominantly expressed in disc cells compared to macrophages in degenerative IVDs in mice.³⁸ In our present study, chondrocytic cells in degenerative IVD were positive for TGF- β . Therefore, chondrocytic cell-derived TGF- β may modulate M2 polarization in degenerative IVDs. However, factors governing the release of TGF- β remain unclear.

Mice IVDs characteristically differ to those of humans. The vertebral column and thus the IVDs of all mammals arise from aggregation of the mesenchyme around the notochord and subsequent segmentation during development.^{39,40} Notochordal cells persist in the NP of mice into adulthood. However, the number of these cells decreases rapidly following birth in humans and notochordal cells are completely absent from the NP by early adulthood. The mice IVDs are also subject to significantly different mechanical loading to human IVDs. In addition, puncturing of IVDs is not exactly the same as IVD degeneration, which is a chronic process. Therefore, experimentation on human IVDs is necessary to validate our mice data.

Conclusion

M2 M ϕ following IVD injury may predominantly originate from resident M ϕ . TGF- β plays a role in M2 polarization.

Authors' contributions

AK, MM, GI, and KU contributed to conception and design of the study. AK and KU wrote the manuscript. AK, MM, YY, MN, ST,

MT and MI participated in the data collection, and did the statistical analysis. AK, MT and KU edited the manuscript. AK and MT oversaw the study. Each author read and approved the final article.

Declaration of conflicting interests

The author(s) declared no potential conflicts of interest with respect to the research, authorship, and/or publication of this article.

Funding

The author(s) disclosed receipt of the following financial support for the research, authorship, and/or publication of this article: This investigation was partly supported by Mitsufumi Nakawaki, Grant-in-Aid for Scientific Research (C) Grant No. 20K09510 and by Masayuki Miyagi, Grant-in-Aid for Research Activity Start-up Grant No. 20K22984.

Ethical approval

The study protocol was approved by the Kitasato Institutional Animal Care Committee (reference number: 2020–089). The study was conducted in accordance with the ARRIVE guidelines for reportage of animal experiments. All methods were performed consistent with guidelines for the proper conduct of animal experiments from the Science Council of Japan.

Data availability

The datasets which support the conclusion of this article are included within the article. The raw data is available for request from the corresponding author.

Animal welfare

The present study followed international, national, and/or institutional guidelines for humane animal treatment and complied with relevant legislation.

ORCID iD

Kentaro Uchida  <https://orcid.org/0000-0001-5148-914X>

Supplemental Material

Supplemental Material for this article is available online.

References

1. Nakazawa KR, Walter BA, Laudier DM, et al. (2018) Accumulation and localization of macrophage phenotypes with human intervertebral disc degeneration. *The Spine Journal* 18: 343–356.
2. Takada T, Nishida K, Doita M, et al. (2004) Interleukin-6 production is upregulated by interaction between disc tissue and macrophages. *Spine (Phila Pa 1976)* 29: 1089–1092. discussion 1093.

3. Takada T, Nishida K, Maeno K, et al. (2012) Intervertebral disc and macrophage interaction induces mechanical hyperalgesia and cytokine production in a herniated disc model in rats. *Arthritis & Rheumatology* 64: 2601–2610.
4. Miyagi M, Uchida K, Takano S, et al. (2018) Macrophage-derived inflammatory cytokines regulate growth factors and pain-related molecules in mice with intervertebral disc injury. *Journal of Orthopaedic Research* 36: 2274–2279.
5. Miyagi M, Uchida K, Takano S, et al. (2020) Role of CD14-positive cells in inflammatory cytokine and pain-related molecule expression in human degenerated intervertebral discs. *Journal of Orthopaedic Research* 39: 1755–1762.
6. Nakawaki M, Uchida K, Miyagi M, et al. (2019) Changes in nerve growth factor expression and macrophage phenotype following intervertebral disc injury in mice. *Journal of Orthopaedic Research* 37: 1798–1804.
7. Kawakubo A, Uchida K, Miyagi M, et al. (2020) Investigation of resident and recruited macrophages following disc injury in mice. *Journal of Orthopaedic Research* 38: 1703–1709.
8. Nakawaki M, Uchida K, Miyagi M, et al. (2020) Sequential CCL2 expression profile after disc injury in mice. *Journal of Orthopaedic Research* 38: 895–901.
9. Davies LC, Jenkins SJ, Allen JE, et al. (2013) Tissue-resident macrophages. *Nature Immunology* 14: 986–995.
10. Gautier EL, Chow A, Spanbroek R, et al. (2012) Systemic analysis of PPAR γ in mouse macrophage populations reveals marked diversity in expression with critical roles in resolution of inflammation and airway immunity. *Journal of Immunology* 189: 2614–2624.
11. Brigitte M, Schilte C, Plonquet A, et al. (2010) Muscle resident macrophages control the immune cell reaction in a mouse model of notexin-induced myoinjury. *Arthritis & Rheumatology* 62: 268–279.
12. Schipper HS, Prakken B, Kalkhoven E, et al. (2012) Adipose tissue-resident immune cells: key players in immunometabolism. *Trends in Endocrinology & Metabolism* 23: 407–415.
13. Mantovani A, Biswas SK, Galdiero MR, et al. (2013) Macrophage plasticity and polarization in tissue repair and remodelling. *Journal of Pathology* 229: 176–185.
14. Mantovani A, Sica A and Locati M (2005) Macrophage polarization comes of age. *Immunity* 23: 344–346.
15. Lee S, Millicamps M, Foster DZ, et al. (2020) Long-term histological analysis of innervation and macrophage infiltration in a mouse model of intervertebral disc injury-induced low back pain. *Journal of Orthopaedic Research* 38: 1238–1247.
16. Chen S, Liu S, Ma K, et al. (2019) TGF- β signaling in intervertebral disc health and disease. *Osteoarthritis and Cartilage* 27: 1109–1117.
17. Nerlich AG, Bachmeier BE and Boos N (2005) Expression of fibronectin and TGF- β 1 mRNA and protein suggest altered regulation of extracellular matrix in degenerated disc tissue. *European Spine Journal* 14: 17–26.
18. Tolonen J, Gronblad M, Virri J, et al. (2001) Transforming growth factor beta receptor induction in herniated intervertebral disc tissue: an immunohistochemical study. *European Spine Journal* 10: 172–176.
19. Uchiyama Y, Guttapalli A, Gajghate S, et al. (2008) SMAD3 functions as a transcriptional repressor of acid-sensing ion channel 3 (ASIC3) in nucleus pulposus cells of the intervertebral disc. *Journal of Bone and Mineral Research* 23: 1619–1628.
20. Wu Q, Wang J, Skubutyte R, et al. (2012) Smad3 controls beta-1,3-glucuronosyltransferase 1 expression in rat nucleus pulposus cells: implications of dysregulated expression in disc disease. *Arthritis & Rheumatology* 64: 3324–3333.
21. Cho H, Lee S, Park SH, et al. (2013) Synergistic effect of combined growth factors in porcine intervertebral disc degeneration. *Connective Tissue Research* 54: 181–186.
22. Xie Z, Jie Z, Wang G, et al. (2018) TGF- β synergizes with ML264 to block IL-1 β -induced matrix degradation mediated by Kruppel-like factor 5 in the nucleus pulposus. *BBA Molecular Basis of Disease* 1864: 579–589.
23. Yang H, Gao F, Li X, et al. (2015) TGF- β 1 antagonizes TNF- α induced up-regulation of matrix metalloproteinase 3 in nucleus pulposus cells: role of the ERK1/2 pathway. *Connective Tissue Research* 56: 461–468.
24. Gratchev A (2017) TGF- β signalling in tumour associated macrophages. *Immunobiology* 222: 75–81.
25. Tsunawaki S, Sporn M, Ding A, et al. (1988) Deactivation of macrophages by transforming growth factor- β . *Nature* 334: 260–262.
26. Yokozeki Y, Kawakubo A, Miyagi M, et al. (2021) Reduced TGF- β expression and CD206-positive resident macrophages in the intervertebral discs of aged mice. *BioMed Research International* 2021: 7988320.
27. Cao Q, Wang Y, Zheng D, et al. (2010) IL-10/TGF- β -modified macrophages induce regulatory T cells and protect against adriamycin nephrosis. *Journal of the American Society of Nephrology* 21: 933–942.
28. Davies MR, Liu X, Lee L, et al. (2016) TGF- β small molecule inhibitor SB431542 reduces rotator cuff muscle fibrosis and fatty infiltration by promoting fibro/adipogenic progenitor apoptosis. *PLoS One* 11: e0155486.
29. Lemos DR, Babaeijandaghi F, Low M, et al. (2015) Nilotinib reduces muscle fibrosis in chronic muscle injury by promoting TNF-mediated apoptosis of fibro/adipogenic progenitors. *Nature Medicine* 21: 786–794.
30. Kadomoto S, Izumi K and Mizokami A (2021) Macrophage polarity and disease control. *International Journal of Molecular Sciences* 23(1): 144.
31. Lurier EB, Dalton D, Dampier W, et al. (2017) Transcriptome analysis of IL-10-stimulated (M2c) macrophages by next-generation sequencing. *Immunobiology* 222: 847–856.

32. Spiller KL, Anfang RR, Spiller KJ, et al. (2014) The role of macrophage phenotype in vascularization of tissue engineering scaffolds. *Biomaterials* 35: 4477–4488.
33. Spiller KL, Nassiri S, Witherell CE, et al. (2015) Sequential delivery of immunomodulatory cytokines to facilitate the M1-to-M2 transition of macrophages and enhance vascularization of bone scaffolds. *Biomaterials* 37: 194–207.
34. Nerlich AG, Weiler C, Zipperer J, et al. (2002) Immunolocalization of phagocytic cells in normal and degenerated intervertebral discs. *Spine (Phila Pa 1976)* 27: 2484–2490.
35. Tolonen J, Gronblad M, Vanharanta H, et al. (2006) Growth factor expression in degenerated intervertebral disc tissue. An immunohistochemical analysis of transforming growth factor beta, fibroblast growth factor and platelet-derived growth factor. *European Spine Journal* 15: 588–596.
36. Zahner SP, Kel JM, Martina CA, et al. (2011) Conditional deletion of TGF-betaR1 using Langerin-Cre mice results in Langerhans cell deficiency and reduced contact hypersensitivity. *Journal of Immunology* 187: 5069–5076.
37. Standiford TJ, Kuick R, Bhan U, et al. (2011) TGF-beta-induced IRAK-M expression in tumor-associated macrophages regulates lung tumor growth. *Oncogene* 30: 2475–2484.
38. Yokozeki Y, Uchida K, Kawakubo A, et al. (2021) TGF-beta regulates nerve growth factor expression in a mouse intervertebral disc injury model. *BMC Musculoskeletal Disorders* 22: 634.
39. Alini M, Eisenstein SM, Ito K, et al. (2008) Are animal models useful for studying human disc disorders/degeneration? *European Spine Journal* 17: 2–19.
40. Daly C, Ghosh P, Jenkin G, et al. (2016) A review of animal models of intervertebral disc degeneration: pathophysiology, regeneration, and translation to the clinic. *BioMed Research International* 2016: 5952165.